Chemical Science

ROYAL SOCIETY OF CHEMISTRY

EDGE ARTICLE

View Article Online
View Journal | View Issue

Cite this: *Chem. Sci.*, 2025, **16**, 16729

All publication charges for this article have been paid for by the Royal Society of Chemistry

Received 28th March 2025
Accepted 11th August 2025

DOI: 10.1039/d5sc02374b

rsc.li/chemical-science

Correlation-driven charge migration triggered by infrared multi-photon ionization

Clément Guiot du Doignon, Rajarshi Sinha-Roy, * Franck Rabilloud and Victor Despré *

The possibility of observing correlation-driven charge migration has been a driving force behind theoretical and experimental developments in the field of attosecond molecular science since its inception. Despite significant accomplishments, the unambiguous experimental observation of this quantum beating remains elusive. In this work, we present a method to selectively trigger such dynamics in molecules predicted to exhibit long-lived electron coherence. We show that these dynamics can be selectively triggered using infrared multi-photon ionization and probed using the spacial resolution of X-ray free-electron laser, proposing a promising experimental scheme to study these pivotal dynamics. Additionally, we demonstrate that real-time time-dependent density-functional theory can describe correlation-driven charge migration resulting from a hole mixing structure involving the highest occupied molecular orbital of a molecule.

Introduction

The development of ultrafast technologies, which permit the study of matter down to the attosecond (as) time scale (10^{-18}),[1,2] has enabled the investigation of fundamental quantum effects that were previously inaccessible.[3,4] In molecular physics, this was first demonstrated through experiments on the fragmentation of H_2 (ref. 5) and the ionization of small polyatomic molecules.[6] Currently, the attosecond community aims to expand the application of ultrafast technologies into new research fields. For example, nowadays it has become possible to use extreme ultraviolet (XUV) pulses as a trigger on biologically relevant systems.[7] Also its use on carbon based structures like polycyclic aromatic hydrocarbons is shedding new light on questions relevant to astrochemistry.[8]

These advancements have often been driven and supported by new theoretical developments and ideas. One significant theoretical prediction that propelled the early development of attosecond technologies is the correlation-driven charge migration,[9] as predicted by Lorenz Cederbaum.[10] Referred to as "the holy grail of attosecond molecular physics",[11] charge migration involves ultrafast purely electron dynamics resulting from the coherent superposition of eigenstates in a molecular system. This should be distinguished from charge transfer dynamics, which are driven by nuclear motion. Correlation-driven charge migration specifically refers to phenomena where the aforementioned superposition can be created by ionizing a single molecular orbital, a process made possible by electron correlation.[12] This arises from the presence of so-called correlation structures (hole mixing and satellites) in the ionization spectrum of molecules. These structures are due to the electron correlation, as they would not exist at the Hartree–Fock level, which is why the term 'correlation-driven' is used. Investigating correlation-driven charge migration provides a direct and insightful way to study electron correlation, which is one of the primary goals of attosecond science.

However, despite significant theoretical[13–24] and experimental[7,25–28] efforts, the unambiguous observation of correlation-driven charge migration, or more generally, charge migration dynamics triggered by ionization, remains elusive. Recently, X-ray free-electron lasers have emerged as a particularly promising tool for experimentally observing correlation-driven charge migration.[29–31] These large-scale infrastructures offer the exciting possibility of probing the charge distribution within a molecule at the atomic level by exploiting the spacial resolution of X-ray photons, potentially making the experimental observation of this long-sought-after phenomenon a reality.

Pursuing such an observation is crucial as charge migration is central to extending attosecond technologies into chemistry, a field referred to as attochemistry. The goal is to steer the chemical reactivity of a molecular system by controlling its purely electron dynamics, the charge migration. The study of attochemistry is timely, as two of its prerequisites have been demonstrated: the existence of long-lived electron coherence, as observed for neutral silane,[32] and the impact of pure electron dynamics on the reactivity of a molecular system, as demonstrated for adenine.[33,34] In this context, ionization-triggered

Université Claude Bernard Lyon 1, CNRS, Institut Lumière Matière, UMR5306, F-69100 Villeurbanne, France. E-mail: rajarshi.sinha-roy@univ-lyon1.fr; victor.despre@univ-lyon1.fr

dynamics are particularly interesting as they allow control over the created hole in the system, directly influencing molecular reactivity.[35]

A potential obstacle in observing ionization-induced charge migration is the decoherence of the superposition of states created during the process, first discussed in the context of the benzene molecule.[36] Predictions have been made for both long-lived coherence[36,37] (around 15 fs, representing several periods of charge migration) and extremely short coherence (1–2 fs, which is only a fraction of the charge migration period).[38–40] Long-lived coherence has predominantly been predicted for correlation-driven charge migration.[36,37,41] These studies have shown that long-lived coherence is achievable, but for that selecting appropriate systems is crucial. Current efforts aim to better understand which systems are likely to exhibit long-lived coherence,[40] potentially leading to the design of molecules with interesting long-lived charge migration dynamics.[42–45] Despite identifying promising molecular systems, no direct experimental observation of the correlation-driven charge migration has been made yet, raising questions about other possible barriers.

Experimental attempts to observe charge migration have mostly employed XUV-pump infrared (IR)-probe schemes.[7,25] However, the lack of selectivity of the pump could be a limiting factor. An XUV-pump will populate all cationic eigenstates of a molecule, as the pump spectrum usually extends beyond the double ionization threshold of most molecules. Consequently, the charge migration dynamics may not be efficiently populated or discernible from the experimental data. Nevertheless, the XUV-pump IR-probe scheme has achieved significant success, particularly in studying states just below the double ionization threshold of molecules,[8,46] where the breakdown of the molecular picture[47] creates a correlation band.[48–50]

In this work, we propose a different approach to trigger correlation-driven charge migration with strong selectivity. Multi-photon IR excitation is known to ionize a limited number of the outermost molecular orbitals, as demonstrated by above-threshold ionization experiments.[51,52] Using intense IR pulses as a trigger will dramatically limit the number of populated cationic eigenstates. The question is how to trigger correlation-driven charge migration this way. We propose selecting molecular systems with a hole mixing structure for their highest occupied molecular orbital (HOMO). A hole mixing structure consists of two or more cationic states described by contributions from two or more different orbitals.[12] In the case of two states and two orbitals, ionizing one of the orbitals involved in the mixing will populate both states, with their populations determined by the corresponding weight of the orbitals in each state. Such hole mixing for the HOMO is not rare, as demonstrated by seminal works of the Heidelberg group on PENNA[53] and MePeNNA.[54] Long-lived electron coherences have also been predicted for such structures, first for propiolic acid with a quantum treatment of both electronic and nuclear degrees of freedom,[37] coherence time that may even be controlled,[55] and then for but-3-ynal, 2,5-dihydrofuran, and 3-pyrroline with a semi-classical approach.[41] These four molecules will be studied in this paper.

To simulate correlation-driven charge migration triggered by IR multiphoton ionization, the theoretical approach must meet several constraints. It must accurately describe not only the states involved in the desired coherent superposition but also their population following ionization by attosecond-to-few-femtosecond pulses. It must therefore handle ionization and provide a high level of electron correlation treatment to describe hole mixing structures accurately. Real-time time-dependent density functional theory (RT-TDDFT) in its real-space formulation shows promise due to its unique ability to explicitly treat the ionization step, a capability lacking in the majority of other methods that rely on sudden ionization. RT-TDDFT was first shown to be relevant for attosecond science by simulating the control of XUV ionization induced by an IR polarizing pulse for N_2, CO_2, and C_2H_4,[6] and has since been used regularly in various studies[56–59] even in the context of strong field ionization.[60] It handles ionization by adding absorbing boundaries at the simulation box's limits. While the ionization criterion is met, the question remains whether RT-TDDFT can properly describe correlation-driven charge migration. This has been addressed in the case of dynamics due to satellite states, where the single determinant nature of TDDFT led to nonphysical behavior due to the importance of multi-excitation for satellites,[61] which is not the case for hole mixing that are characterized by a sum of single excitation, a form similar to that of excited states in TDDFT, as clearly evident in the Casida formalism.[62] Another consideration is how well Kohn–Sham orbitals describe ionization. Koopmans' theorem for the HOMO is favorable,[63] but no such theorem exists for other orbitals.

In this paper, we first show that RT-TDDFT can accurately describe correlation-driven charge migration for propiolic acid, but-3-ynal, 2,5-dihydrofuran, and 3-pyrroline by simulating the sudden ionization of their HOMO. We then demonstrate that short intense IR pulses can selectively trigger these dynamics, proposing a novel approach for the experimental observation of correlation-driven charge migration.

Results and discussion

Simulations were performed using the open-source code octopus, which allows RT-TDDFT simulations in real space, *i.e.*, on a grid.[64,65] This approach offers the advantage of straightforward convergence of the ionization process by increasing both the size of the simulation box and of the absorbing boundaries. All simulations presented in this paper are done using the adiabatic approximation with the gradient corrected PBE functional.[66] In addition, to correct the self-interaction error (SIE) so that the asymptotic behavior of the effective potential can be properly described, a scheme[67,68] based on the average density is used. The dependence of the predicted dynamics on the functional used will be discussed later. The correction of the SIE significantly improves the ionization potential of the molecules, thereby enhancing the description of ionization. Simulations were conducted on a spherical grid with a radius of 12 Å, a spacing of 0.18 Å, and a time step of 1.3 as. Absorbing boundaries with a thickness of 2 Å were used at the edge of the spherical simulation domain. All these

parameters were optimized by incrementally refining them until no noticeable changes in the results were observed. These parameters depend on the properties of the laser pulses used and should be carefully re-evaluated when different laser conditions are considered. This is partly because different laser parameters result in the emission of photoelectrons with varying kinetic energies, which interact differently with the absorbing boundaries. For consistency, all computations were therefore performed using the stricter set of parameters. The molecular geometries used in this study can be found in the SI.

The first step of our study involved simulating correlation-driven charge migration resulting from the sudden ionization of the HOMO of the four molecules to evaluate the capability of RT-TDDFT simulations. To achieve this, an electron was removed from their HOMO at the start of the simulations ($t = 0$). The results, presented in Fig. 1, can be compared to dynamics predicted using high-level *ab initio* method, the algebraic diagrammatic construction at third order (ADC(3)),[69,70] as presented in ref. 37 for propiolic acid and ref. 41 for but-3-ynal, 2,5-dihydrofuran, and 3-pyrroline. In Fig. 1, the time-dependent hole density is projected along the molecular axis (the x axis), meaning it is integrated over planes perpendicular to this axis. This is illustrated by the molecular orientation shown in the leftmost column and the coordinate axes in the bottom-right corner of the figure. The labels H, C, O, and N denotes respectively the x – component of the position of the hydrogen, carbon, oxygen, and the nitrogen atoms. The hole density represents the difference between the electron density of the neutral system and the time-dependent electron density of the cationic system. Since the simulations do not account for nuclear dynamics or ionized electrons, decoherence is absent, and pure electron dynamics is maintained throughout.

Strong charge migration dynamics, similar to those predicted with ADC(3),[37,41] are observed in all systems. These dynamics result from a hole-mixing structure that enables the coherent population of multiple states through the ionization of a single molecular orbital. For example, this is clearly seen in the case of the propiolic acid molecule (top panel of Fig. 1),

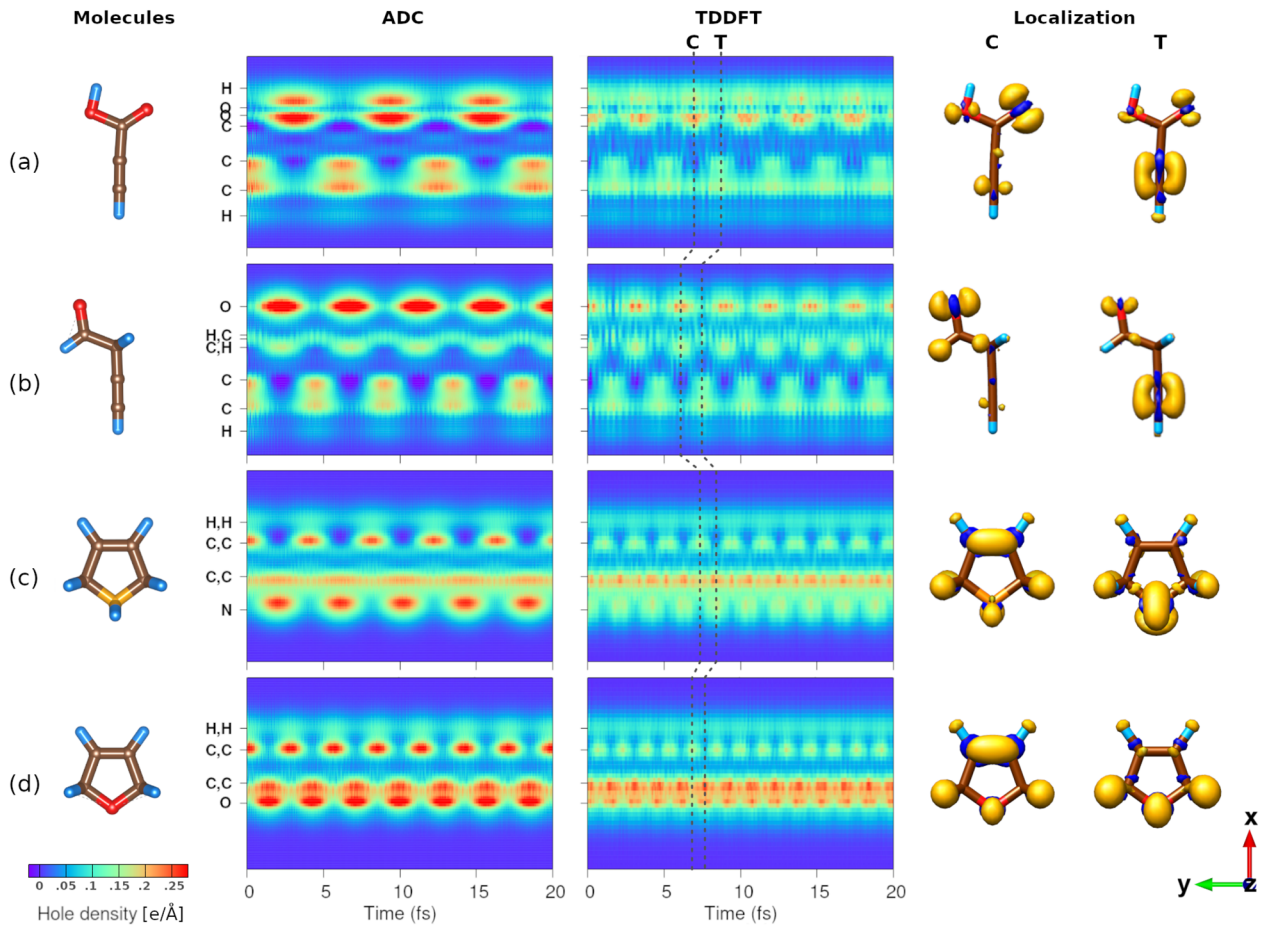

Fig. 1 The time-dependent oscillation of the hole density projected along the molecular axis due to the sudden ionization of the HOMO of propiolic acid (a), but-3-ynal (b), 3-pyrroline (c), and 2,5-dihydrofuran (d) is shown through color maps. The left-most column shows the molecules with their molecular axes oriented along the x-axis (*cf.*, axes arrows). The third column represents calculations using TDDFT and compares to the results obtained in ADC as shown in the second one. The values of the hole density are represented by the color bar (a negative hole density means an excess of electron). For the TDDFT results, the localization of the hole-density corresponding to a crests (C) and a trough (T) of the oscillatory dynamics is presented as iso-surface in the last two columns. The iso-values are 0.005 e Å^{-3} for (a) and (b), and 0.008 e Å^{-3} for (c) and (d).

where the generated hole (in red) moves from the carbon triple bond to the oxygen atoms. A similarity in the shape of the time-dependent hole density for the four molecules can be observed. For all systems, a major part of the dynamics involves the migration of charge between an oxygen or nitrogen atom and a carbon–carbon triple or double bond. Periods of approximately 3.3 fs for propiolic acid, 2.9 fs for but-3-ynal, 2 fs for 3-pyrroline, and 1.55 fs for 2,5-dihydrofuran are predicted. These can be compared with periods of 6.2 fs for propiolic acid, 4.5 fs for but-3-ynal, 4 fs for 3-pyrroline, and 2.8 fs for 2,5-dihydrofuran predicted using ADC(3). The periods are obtained from the Fourier analysis of the simulated dynamics in RT-TDDFT, following the concept proposed by Yabana and co-workers,[71,72] and directly from the state energies in the ADC(3) simulations. The difference in periods calculated in the two different levels of theory is not surprising, it depends solely on the energy gap between the states in the coherent superposition, and these energies can vary depending on the level of theory used. In fact, a difference in the energy gap of just around 0.59 eV accounts for the largest observed difference in period, *i.e.*, for the case of propiolic acid. The strengths of the localization of the charge also differ between the TDDFT and ADC(3) simulations. It depends on the overlap between the states in the superposition, a stronger overlap leads to stronger charge localization. In the context of hole mixing, a stronger hole-mixing interaction results in states that are more similar and closer in energy. Consequently, slower dynamics generally lead to greater localization, while faster dynamics result in reduced localization. This trend is observed in our results, where TDDFT predicts slightly less localization compared to ADC(3).

Despite the difference in the period and in the strength of the charge localization predicted by RT-TDDFT from that predicted by ADC(3), it is noteworthy how accurately RT-TDDFT describes correlation-driven charge migration resulting from a hole mixing structure. It is essential for RT-TDDFT to accurately describe the distribution of electron density, as this is the cornerstone for studying charge dynamics. Notably, even the LDA[73] functional successfully captures the shape of the dynamics (see the SI for the propiolic acid).[74] This is facilitated by the fact that charge localization during the dynamics arises from the overlap between the states in the coherent superposition. Therefore, if RT-TDDFT can accurately describe the individual states, it will also correctly describe the resulting dynamics. In this case, no problematic states, such as charge transfer states, are present, allowing the dynamics to be reliably simulated even using simple approximations like PBE[66] and LDA.[73] This highlights RT-TDDFT's capability to sufficiently account for electron correlation in describing hole mixing structures.

The next step was to investigate how the predicted dynamics could be triggered by ionization using an intense 800 nm IR pulse. The pulse wavelength was chosen to realistically reflect commonly available laser sources within the attosecond science community and was not subject to optimization. To achieve this, a pulse was explicitly introduced into the simulations, which perturbs the ground states of the neutral molecules. A short pulse with a controlled carrier envelop phase (CEP) limits the time for which the intensity is sufficient for multi-photon ionization. The two pulses used are presented in Fig. 2, representing cases with one extremum for the field (even pulse) or two with equal intensity (odd pulse), both of which can be generated experimentally.[75] In the following we will focus on propiolic acid, the only molecule in this study for which long-lived electron coherence has been predicted using a quantum treatment of both electronic and nuclear degrees of freedom[37] for a dynamics that can even be controlled by laser pulses.[76] The polarization of the field is chosen along the y axis as shown in Fig. 1 meaning that the polarization is perpendicular to the molecular axis. The intensity, around 2.5×10^{14} W cm^{-2}, was set to ensure a maximum ionization of 1. This choice was made to ensure that the results are comparable to those obtained using sudden ionization of a single electron, and to demonstrate that it is not necessary to treat laser intensity as a free parameter to observe the desired dynamics. The level of ionization is determined by the difference between the initial charge within the simulation box and the final charge after part of the electron density passes through the absorbing boundaries. We would like to mention that the laser intensities used in the simulations are not directly transferable to experimental conditions due to factors such as pulse focusing and molecular gas diffusion, which cause the molecules to experience a range of intensities.

As shown in Fig. 2, both laser pulses trigger dynamics similar to those observed with sudden ionization, particularly in the carbon triple bond region. This indicates that the correlation-driven charge migration dynamics are efficiently and selectively initiated. As expected, a small difference in frequency is observed due to propagation under two different Hamiltonians, the N-electron and the $(N-1)$-electron systems, as shown by the Fourier analysis in Fig. 2. This difference may arise either from a physical effect or from known shortcomings of RT-TDDFT, such as peak-shifting.[77] Importantly, the difference is smaller than the expected precision of RT-TDDFT in this context. It is remarkable how accurately RT-TDDFT predicts correlation-driven charge migration resulting from a hole mixing involving the HOMO, even in the presence of a strong field. However, the dynamics induced by the odd pulse appear more blurred due to significant population of higher-lying cationic states resulting from excitation of the cation during the pulse. This suggests that coherent control occurs during the pulse itself. This is further confirmed by the Fourier analysis shown in the right column of Fig. 2, where strong signals are observed at both key sites of the dynamics—the carbon triple bond and the oxygen atoms. These secondary dynamics, which strongly localizes the hole around the singly bounded oxygen, becomes dominant for certain orientations. This means that, although the desired dynamics may still be somewhat observable for a specific orientation, the pulse does not appear suitable for experimental observation of the dynamics. Therefore, the even pulse appears to be more suitable for triggering the desired dynamics, indicating that the choice of the CEP is a crucial parameter for the experimental observation of these dynamics.

Ultrafast beatings are also observed, resulting from the ionization of other orbitals, particularly HOMO−1 and

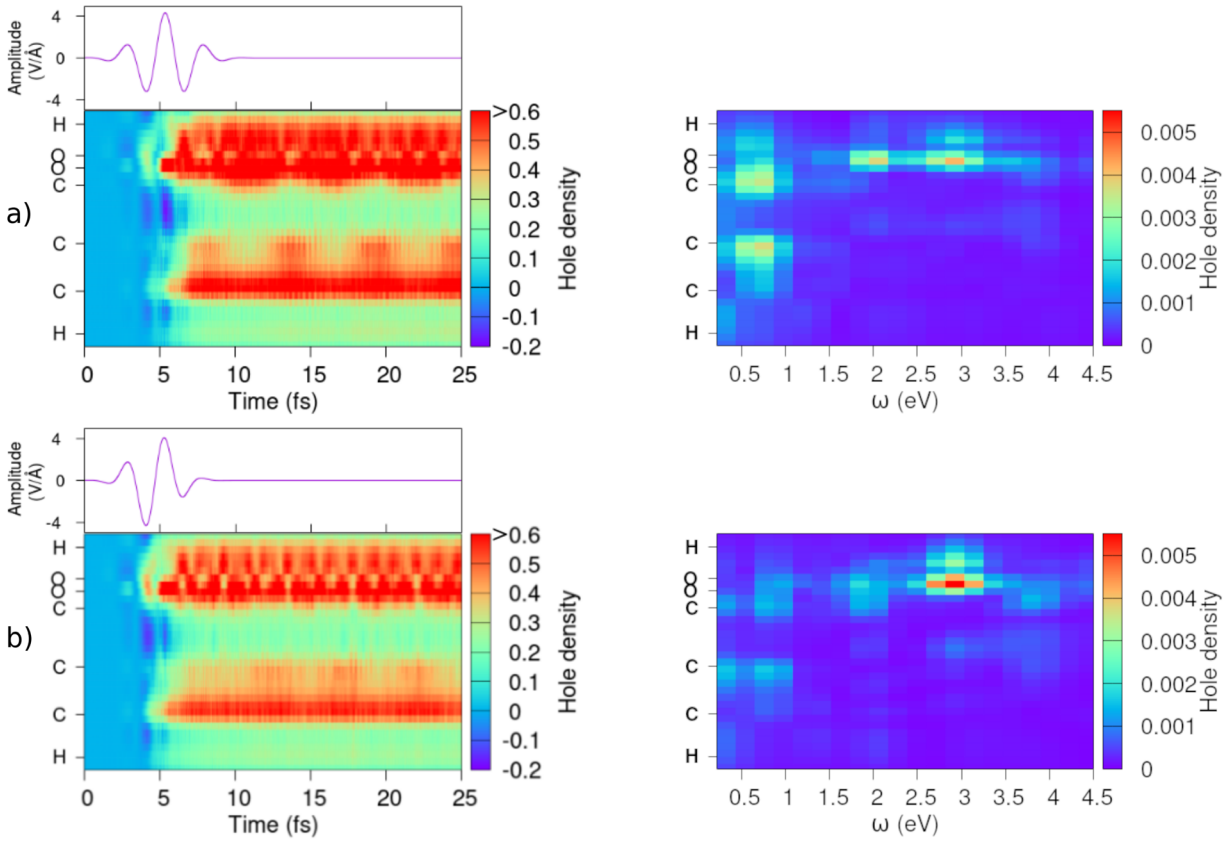

Fig. 2 Time-dependent hole density (left panels) and its Fourier transform (right panels) for propiolic acid projected along the molecular axis, shown as the y-axis of each panel, following multi-photon ionization triggered by an (a) even or (b) odd laser pulse, as illustrated above each panel. The hole density is normalized to its maximum value.

HOMO−2, where sudden ionization leads to such patterns. This effect is partly due to the imperfect description of ionization by Kohn–Sham orbitals, resulting in a nonphysical superposition of states separated by a large energy gap. However, it is striking that the frequency of the correlation-driven charge migration remains strongly present, even in the region of the oxygen atoms, as shown in the Fourier analysis. Longer pulses were tested and also triggered the desired dynamics; however, given that an electron coherence of approximately 15 fs is predicted for the studied molecule, longer pulses are less likely to enable experimental observation of the dynamics.

To guide experiments, we investigated whether molecular orientation is necessary for the experimental observation of the dynamics. We used the even pulse shown in Fig. 3, with an intensity around 1.6×10^{14} W cm^{-2} and averaged the dynamics over 17 different molecular orientations. These results first demonstrate that the dynamics can be observed even with less intense pulses and with varying ionization rates, as the ionization rate depends on the molecular orientation. The choice of the intensity impacts the contrast of the observed dynamics and must be chosen carefully. To better illustrate the impact of laser intensity, a comparison of the resulting dynamics at different pulse intensities is presented in the SI. The chosen orientations included the three principal axes shown in Fig. 1 and their equal combinations, leveraging the molecule's C_s symmetry, which allows us to explore only half of the physical space. The averaged dynamics are shown in (Fig. 3a) for the full averaging and in (Fig. 3b) when only the 8 orientations lying in the plane of the molecule are considered. We found that the dynamics are still observed even with different orientations, though the contrast of spatial charge localization is better when only in-plane orientations are considered. The quality of the contrast in the in-plane averaging results from the fact that the dynamics are triggered across multiple orientations, not just a single specific one. The Fourier analysis in Fig. 3 shows that the frequency of the correlation-driven charge migration is notably present for both averaging cases in both the regions: the oxygen atoms and the carbon triple bond. This suggests that using an intense single-cycle IR pulse with a suitable CEP on randomly oriented molecules will selectively trigger the desired dynamics. While molecular alignment is not mandatory, it can enhance the observation of the dynamics by improving their charge-localization contrast.

A key remaining question is how such dynamics can be effectively probed. One particularly attractive option is the use of X-ray free-electron lasers,[29–31] which have developed technologies capable of being highly sensitive to local processes by leveraging the spacial resolution of core transitions. Correlation-driven charge migration alters the screening of specific atoms within a molecule, leading to changes in core

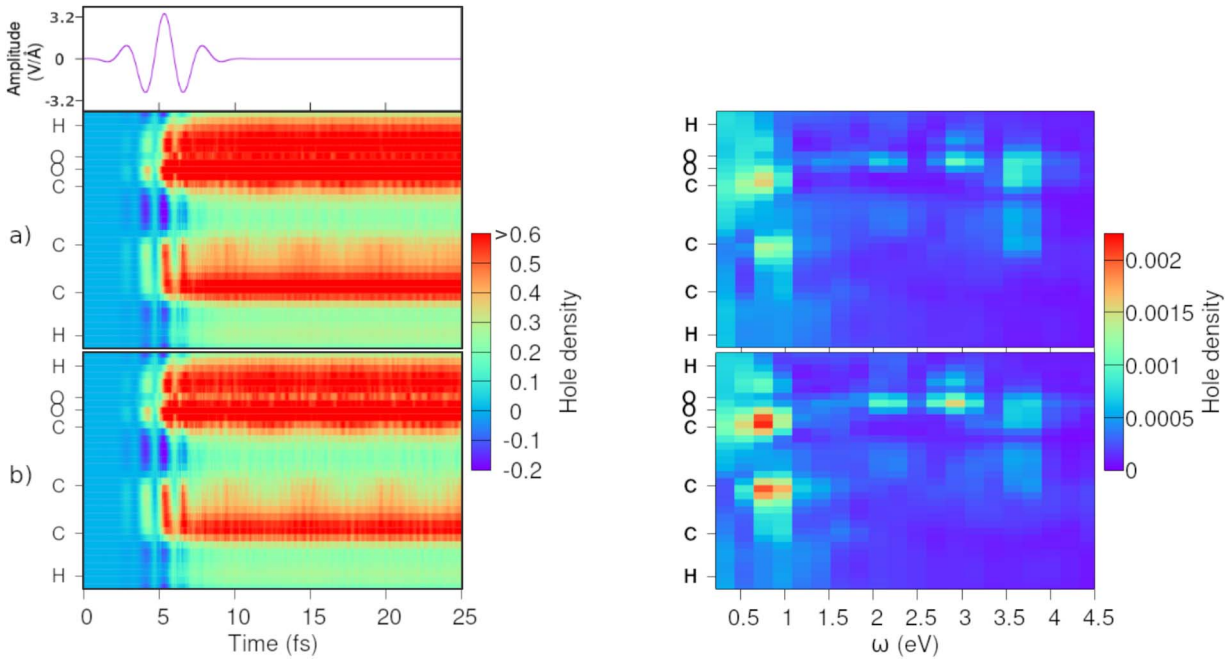

Fig. 3 Time-dependent hole density (left panels) and its Fourier transform (right panels) for propiolic acid projected along the molecular axis, shown as the *y*-axis of each panel, following multi-photon ionization triggered by the even pulse shown above the panels averaged over (a) 17 and (b) 8 orientation (see text). The hole density is normalized to its maximum value.

transitions. This enables the creation of a "molecular movie",[78] allowing to track the movement of the hole within a molecule by probing different atoms. This approach has even been demonstrated theoretically for propiolic acid,[79] where it was shown that the time-resolved absorption cross-section for transitions from the 1s orbitals of carbon and oxygen is influenced by the correlation-driven charge migration occurring within the valence electrons of the molecule. Consequently, an IR-pump/X-ray probe setup at an X-ray free-electron lasers facility appears to be a highly suitable scheme for studying correlation-driven charge migration.

Conclusions

In this paper, we have shown that RT-TDDFT can accurately describe correlation-driven charge migration dynamics resulting from hole mixing structures, even using the simplest functional. The Kohn–Sham HOMO adequately describes ionization, enabling the study of dynamics triggered by ionization with a short, intense IR pulse. We have demonstrated that these dynamics can be selectively triggered, with the choice of CEP and intensity playing a crucial role, while random molecular orientations can still be utilized. The resulting dynamics can then be effectively probed using X-ray free-electron lasers. We have proposed an efficient and selective alternative to using XUV attosecond pulses for triggering charge migration. This elegant method allows for a comprehensive test of the concept of correlation-driven charge migration by creating a situation where it is experimentally possible to limit ionization to a single molecular orbital. This enables the testing of whether pure electron dynamics can indeed be triggered by the ionization of a single molecular orbital. While this approach is limited to systems with a hole mixing structure for the HOMO, such occurrences are not rare, and provide a direct and simple way to study electron coherence by unambiguously investigating the elusive correlation-driven charge migration mechanism. We hope our work will motivate new experiments aimed at observing charge migration dynamics and theoretical studies to deepen our understanding of the opportunities offered by RT-TDDFT in this context.

Author contributions

C. G. d. D. and R. S. R. performed the simulations. V. D. designed and conceptualized the project. F. R. and V. D. supervised the work. All authors contributed to the discussion of the results, provided feedback, and reviewed the manuscript.

Conflicts of interest

There are no conflicts to declare.

Data availability

The octopus code used for the RT-TDDFT simulations is freely available at **https://www.octopus-code.org/documentation/15/**.

Geometries of the studied molecules and dynamics obtained using various exchange–correlation functionals and laser intensities. See DOI: **https://doi.org/10.1039/d5sc02374b**.

Acknowledgements

The authors thank Franck Lépine and Alexander Kuleff for fruitful discussions.

Notes and references

1 P. Antoine, A. L'huillier and M. Lewenstein, *Phys. Rev. Lett.*, 1996, **77**, 1234.
2 F. Krausz and M. Ivanov, *Rev. Mod. Phys.*, 2009, **81**, 163–234.
3 F. Lépine, M. Y. Ivanov and M. J. Vrakking, *Nat. Photonics*, 2014, **8**, 195–204.
4 M. Nisoli, P. Decleva, F. Calegari, A. Palacios and F. Martín, *Chem. Rev.*, 2017, **117**, 10760–10825.
5 G. Sansone, F. Kelkensberg, J. Pérez-Torres, F. Morales, M. F. Kling, W. Siu, O. Ghafur, P. Johnsson, M. Swoboda, E. Benedetti, *et al.*, *Nature*, 2010, **465**, 763–766.
6 C. Neidel, J. Klei, C.-H. Yang, A. Rouzée, M. Vrakking, C. Arnold, *et al.*, *Phys. Rev. Lett.*, 2013, **111**, 033001.
7 F. Calegari, D. Ayuso, A. Trabattoni, L. Belshaw, S. De Camillis, S. Anumula, F. Frassetto, L. Poletto, A. Palacios, P. Decleva, *et al.*, *Science*, 2014, **346**, 336–339.
8 A. Marciniak, V. Despré, G. Karras, M. Hervé, L. Quintard, F. Catoire, C. Joblin, A. Kuleff, *et al.*, *Nat. Commun.*, 2019, **10**, 337.
9 A. I. Kuleff and L. S. Cederbaum, *J. Phys. B:At., Mol. Opt. Phys.*, 2014, **47**, 124002.
10 J. Zobeley and L. S. Cederbaum, *Chem. Phys. Lett.*, 1999, **307**, 205–210.
11 F. Lépine, G. Sansone and M. J. Vrakking, *Chem. Phys. Lett.*, 2013, **578**, 1–14.
12 J. Breidbach and L. Cederbaum, *J. Chem. Phys.*, 2003, **118**, 3983–3996.
13 A. I. Kuleff, S. Lünnemann and L. S. Cederbaum, *J. Phys. Chem. A*, 2010, **114**, 8676–8679.
14 A. I. Kuleff, N. V. Kryzhevoi, M. Pernpointner and L. S. Cederbaum, *Phys. Rev. Lett.*, 2016, **117**, 093002.
15 B. Mignolet, R. D. Levine and F. Remacle, *J. Phys. B:At., Mol. Opt. Phys.*, 2014, **47**, 124011.
16 S. Sun, B. Mignolet, L. Fan, W. Li, R. D. Levine and F. Remacle, *J. Phys. Chem. A*, 2017, **121**, 1442–1447.
17 M. Lara-Astiaso, D. Ayuso, I. Tavernelli, P. Decleva, A. Palacios and F. Martín, *Faraday Discuss.*, 2016, **194**, 41–59.
18 K. Yuan and A. D. Bandrauk, *J. Phys. Chem. A*, 2019, **123**, 1328–1336.
19 A. S. Folorunso, F. Mauger, K. A. Hamer, D. D. Jayasinghe, I. S. Wahyutama, J. R. Ragains, R. R. Jones, L. F. DiMauro, M. B. Gaarde, K. J. Schafer, *et al.*, *J. Phys. Chem. A*, 2023, **127**, 1894–1900.
20 D. Haase, G. Hermann, J. Manz, V. Pohl and J. C. Tremblay, *Symmetry*, 2021, **13**, 205.
21 B. Zhang, Y. Gu, V. M. Freixas, S. Sun, S. Tretiak, J. Jiang and S. Mukamel, *J. Am. Chem. Soc.*, 2024, **146**, 26743–26750.
22 M. Ruberti, P. Decleva and V. Averbukh, *J. Chem. Theory Comput.*, 2018, **14**, 4991–5000.
23 M. Ruberti, *Phys. Chem. Chem. Phys.*, 2019, **21**, 17584–17604.
24 M. Ruberti, *Faraday Discuss.*, 2021, **228**, 286–311.
25 M. Lara-Astiaso, M. Galli, A. Trabattoni, A. Palacios, D. Ayuso, F. Frassetto, L. Poletto, S. De Camillis, J. Greenwood, P. Decleva, I. Tavernelli, F. Calegari, M. Nisoli and F. Martín, *J. Phys. Chem. Lett.*, 2018, **9**, 4570–4577.
26 P. M. Kraus, B. Mignolet, D. Baykusheva, A. Rupenyan, L. Horný, E. F. Penka, G. Grassi, O. I. Tolstikhin, J. Schneider, F. Jensen, *et al.*, *Science*, 2015, **350**, 790–795.
27 D. Schwickert, M. Ruberti, P. Kolorenč, S. Usenko, A. Przystawik, K. Baev, I. Baev, M. Braune, L. Bocklage, M. K. Czwalinna, *et al.*, *Sci. Adv.*, 2022, **8**, eabn6848.
28 T. Driver, Z. Guo, E. Isele, G. Grell, M. Ruberti, J. T. ONeal, O. Alexander, S. Beauvarlet, D. Cesar, J. Duris *et al.*, *arXiv*, 2024, preprint, arXiv:2411.01700, DOI: **10.48550/arXiv.2411.01700**.
29 S. Li, L. Lu, S. Bhattacharyya, C. Pearce, K. Li, E. T. Nienhuis, G. Doumy, R. Schaller, S. Moeller, M.-F. Lin, *et al.*, *Science*, 2024, **383**, 1118–1122.
30 Z. Guo, T. Driver, S. Beauvarlet, D. Cesar, J. Duris, P. L. Franz, O. Alexander, D. Bohler, C. Bostedt, V. Averbukh, *et al.*, *Nat. Photonics*, 2024, **18**, 691–697.
31 T. Driver, M. Mountney, J. Wang, L. Ortmann, A. Al-Haddad, N. Berrah, C. Bostedt, E. G. Champenois, L. F. DiMauro, J. Duris, *et al.*, *Nature*, 2024, **632**, 762–767.
32 D. T. Matselyukh, V. Despré, N. V. Golubev, A. I. Kuleff and H. J. Wörner, *Nat. Phys.*, 2022, **18**, 1206–1213.
33 E. P. Månsson, S. Latini, F. Covito, V. Wanie, M. Galli, E. Perfetto, G. Stefanucci, H. Hübener, U. De Giovannini, M. C. Castrovilli, *et al.*, *Commun. Chem.*, 2021, **4**, 73.
34 V. Despré and A. I. Kuleff, *Phys. Rev. A*, 2022, **106**, L021501.
35 F. Remacle, R. Levine and M. Ratner, *Chem. Phys. Lett.*, 1998, **285**, 25–33.
36 V. Despré, A. Marciniak, V. Loriot, M. Galbraith, A. Rouzée, M. Vrakking, F. Lépine and A. Kuleff, *J. Phys. Chem. Lett.*, 2015, **6**, 426–431.
37 V. Despré, N. V. Golubev and A. I. Kuleff, *Phys. Rev. Lett.*, 2018, **121**, 203002.
38 M. Vacher, M. J. Bearpark, M. A. Robb and J. P. Malhado, *Phys. Rev. Lett.*, 2017, **118**, 083001.
39 C. Arnold, O. Vendrell and R. Santra, *Phys. Rev. A*, 2017, **95**, 033425.
40 J. Vester, V. Despré and A. Kuleff, *J. Chem. Phys.*, 2023, **158**, 104305.
41 A. Scheidegger, J. Vaníček and N. V. Golubev, *J. Chem. Phys.*, 2022, **156**, 034104.
42 V. Despré and A. I. Kuleff, *Theor. Chem. Acc.*, 2019, **138**, 1–6.
43 A. S. Folorunso, A. Bruner, F. Mauger, K. A. Hamer, S. Hernandez, R. R. Jones, L. F. DiMauro, M. B. Gaarde, K. J. Schafer and K. Lopata, *Phys. Rev. Lett.*, 2021, **126**, 133002.
44 K. Chordiya, V. Despré, B. Nagyillés, F. Zeller, Z. Diveki, A. I. Kuleff and M. U. Kahaly, *Phys. Chem. Chem. Phys.*, 2023, **25**, 4472–4480.
45 E. Belles, F. Rabilloud, A. I. Kuleff and V. Despré, *J. Phys. Chem. A*, 2023, **128**, 163–169.

46 L. Belshaw, F. Calegari, M. J. Duffy, A. Trabattoni, L. Poletto, M. Nisoli and J. B. Greenwood, *J. Phys. Chem. Lett.*, 2012, **3**, 3751–3754.
47 L. S. Cederbaum, W. Domcke, J. Schirmer and W. v. Niessen, *Adv. Chem. Phys.*, 1986, 115–159.
48 M. S. Deleuze and L. S. Cederbaum, *Phys. Rev. B:Condens. Matter Mater. Phys.*, 1996, **53**, 13326.
49 M. Hervé, V. Despré, P. Castellanos Nash, V. Loriot, A. Boyer, A. Scognamiglio, G. Karras, R. Brédy, E. Constant, A. Tielens, *et al.*, *Nat. Phys.*, 2021, **17**, 327–331.
50 A. Boyer, M. Hervé, V. Despré, P. C. Nash, V. Loriot, A. Marciniak, A. Tielens, A. Kuleff and F. Lépine, *Phys. Rev. X*, 2021, **11**, 041012.
51 J. H. Eberly, J. Javanainen and K. Rzążewski, *Phys. Rep.*, 1991, **204**, 331–383.
52 D. Milošević, G. Paulus, D. Bauer and W. Becker, *J. Phys. B:At., Mol. Opt. Phys.*, 2006, **39**, R203.
53 S. Lünnemann, A. I. Kuleff and L. S. Cederbaum, *Chem. Phys. Lett.*, 2008, **450**, 232–235.
54 S. Lünnemann, A. I. Kuleff and L. S. Cederbaum, *J. Chem. Phys.*, 2008, **129**, 104305.
55 D. Dey, A. I. Kuleff and G. A. Worth, *Phys. Rev. Lett.*, 2022, **129**, 173203.
56 M. Lucchini, S. A. Sato, A. Ludwig, J. Herrmann, M. Volkov, L. Kasmi, Y. Shinohara, K. Yabana, L. Gallmann and U. Keller, *Science*, 2016, **353**, 916–919.
57 N. Tancogne-Dejean, O. D. Mücke, F. X. Kärtner and A. Rubio, *Phys. Rev. Lett.*, 2017, **118**, 087403.
58 C.-Z. Gao, P. M. Dinh, P.-G. Reinhard and E. Suraud, *Phys. Chem. Chem. Phys.*, 2017, **19**, 19784–19793.
59 A. Bruner, S. Hernandez, F. Mauger, P. M. Abanador, D. J. LaMaster, M. B. Gaarde, K. J. Schafer and K. Lopata, *J. Phys. Chem. Lett.*, 2017, **8**, 3991–3996.
60 K. A. Hamer, F. Mauger, K. Lopata, K. J. Schafer and M. B. Gaarde, *Phys. Rev. A*, 2025, **111**, L011101.
61 A. I. Kuleff and A. Dreuw, *J. Chem. Phys.*, 2009, **130**, 034102.
62 M. E. Casida, in *Recent Advances In Density Functional Methods: (Part I)*, World Scientific, 1995, pp. 155–192.
63 M. A. L. Marques, *Time-dependent density functional theory*, Springer Science & Business Media, 2006, vol. 706.
64 X. Andrade, D. Strubbe, U. De Giovannini, A. H. Larsen, M. J. Oliveira, J. Alberdi-Rodriguez, A. Varas, I. Theophilou, N. Helbig, M. J. Verstraete, *et al.*, *Phys. Chem. Chem. Phys.*, 2015, **17**, 31371–31396.
65 N. Tancogne-Dejean, M. J. Oliveira, X. Andrade, H. Appel, C. H. Borca, G. Le Breton, F. Buchholz, A. Castro, S. Corni, A. A. Correa, *et al.*, *J. Chem. Phys.*, 2020, **152**, 124119.
66 J. P. Perdew, K. Burke and M. Ernzerhof, *Phys. Rev. Lett.*, 1996, **77**, 3865.
67 C. Legrand, E. Suraud and P. Reinhard, *J. Phys. B:At., Mol. Opt. Phys.*, 2002, **35**, 1115.
68 P. Klüpfel, P. M. Dinh, P.-G. Reinhard and E. Suraud, *Phys. Rev. A:At., Mol., Opt. Phys.*, 2013, **88**, 052501.
69 J. Schirmer, *Phys. Rev. A:At., Mol., Opt. Phys.*, 1982, **26**, 2395.
70 J. Schirmer, *Many-body methods for atoms, molecules and clusters*, Springer, 2018.
71 K. Yabana and G. Bertsch, *Phys. Rev. B:Condens. Matter Mater. Phys.*, 1996, **54**, 4484.
72 K. Yabana, T. Nakatsukasa, J.-I. Iwata and G. Bertsch, *Phys. Status Solidi B*, 2006, **243**, 1121–1138.
73 W. Kohn and L. J. Sham, *Phys. Rev.*, 1965, **140**, A1133–A1138.
74 R. Sinha-Roy, C. Guiot du Doignon, F. Rabilloud and V. Despré, (work in progress).
75 W. A. Okell, T. Witting, D. Fabris, D. Austin, M. Bocoum, F. Frank, A. Ricci, A. Jullien, D. Walke, J. P. Marangos, *et al.*, *Opt. Lett.*, 2013, **38**, 3918–3921.
76 N. V. Golubev, V. Despré and A. I. Kuleff, *J. Mod. Opt.*, 2017, **64**, 1031–1041.
77 X. Li, N. Govind, C. Isborn, A. E. DePrince III and K. Lopata, *Chem. Rev.*, 2020, **120**, 9951–9993.
78 H. Yong, S. Sun, B. Gu and S. Mukamel, *J. Am. Chem. Soc.*, 2022, **144**, 20710–20716.
79 N. V. Golubev, J. Vaníček and A. I. Kuleff, *Phys. Rev. Lett.*, 2021, **127**, 123001.